Dorsomedial prefrontal cortex activity during learning discriminates response to Cognitive Behavioural Therapy in depression.

Filippo Queirazza[1,*], Elsa Fouragnan[1,2], J. Douglas Steele[3], Jonathan Cavanagh[4,5] and Marios G. Philiastides[1,5,*]

Affiliations:

[1]Institute of Neuroscience & Psychology, University of Glasgow, Glasgow, UK

[2]Department of Experimental Psychology, University of Oxford, Oxford, UK

[3]Division of Neuroscience, University of Dundee, Dundee, UK

[4]Sackler Centre for Psychobiological Research, Institute of Health & Wellbeing, University of Glasgow, Glasgow, UK

[5]Co-senior author

***Correspondence:** f.queirazza.1@research.gla.ac.uk; Marios.Philiastides@gla.ac.uk

Institute of Neuroscience & Psychology, 58 Hillhead street, University of Glasgow, Glasgow, UK, G12 8QB

Number of words (Abstract): 244

Number of words (Main text): 4000

Number of figures: 7

Number of supplemental information: 1

Keywords: depression; self-help CBT; fMRI; computational psychiatry; reinforcement learning.

26

27 **Short title:**

28 Predictors of CBT response in depression

29

ABSTRACT

BACKGROUND: Cognitive behavioural therapy (CBT) is an effective evidence based treatment for depression. At present there is no reliable predictor of CBT in depression. Although the key to successful CBT in depression lies in altering maladaptive information processing, no previous imaging study has probed predictors of CBT response using pre-treatment neural encoding of information processing.

METHODS: Using functional magnetic resonance imaging we scanned 37 unmedicated depressed subjects before and after completing computerised CBT (cCBT). We model the trial-by-trial appraisal of feedback information during a probabilistic learning task by means of a dynamic learning rate. To discriminate response to cCBT we capitalise on the pre-treatment blood oxygen level dependent (BOLD) activity encoding the dynamic learning rate as a function of feedback congruence and valence. Additionally, we probe between-group differences in the learning style encoded in the model's parameters.

RESULTS: We show BOLD activity in the dorsomedial prefrontal cortex (dmPFC) to be encoding the dynamic learning rate. Crucially, responders exhibit greater BOLD activity in the dmPFC during incongruent negative trials but lower BOLD activity during congruent negative trials than non-responders. Additionally, on between-group comparisons of model's parameter estimates we show responders take relatively greater account of previous feedback history and make comparatively smaller adjustments to the learning rate as a result of outcome surprisingness.

CONCLUSIONS: Our findings provide novel and important insights into the cognitive mechanisms underpinning response to cCBT and lend support to the feasibility and validity of neurocomputational approaches to treatment prediction research in psychiatry.

Keywords: depression; self-help CBT**;** fMRI; computational psychiatry; reinforcement learning; dynamic learning rate.

INTRODUCTION

The cognitive model of depression posits that biased acquisition and processing of feedback information gives rise to and perpetuates depressive symptoms (1, 2). Based on this theoretical formulation, Aaron T. Beck developed Cognitive Behavioural therapy (CBT) as a treatment for depression (3). CBT is an effective evidence-based intervention for depressive disorder (4, 5). In the UK computerised CBT (cCBT) (that is, self-help internet-delivered CBT) is recommended as a treatment option for mild to moderate depression in the National Institute for Health and Care Excellence guidelines.

Despite recent multidisciplinary efforts (6-12), there is no reliable predictor of clinical response to CBT in depression (13, 14). Neural predictors using functional magnetic resonance imaging (fMRI) provide the additional advantage of illuminating the functional neuroanatomy that underpins response to CBT in depression (15).

Remarkably, although the clinical practice of CBT in depression primarily involves evaluating and ultimately correcting negatively biased inferences drawn from probabilistic information, only emotion eliciting (6, 16, 17) or task-free resting-state paradigms (8, 18, 19) have so far been employed to probe pre-treatment fMRI predictors of CBT response.

In contrast, the computational framework of value-based learning (also known as reinforcement learning) paradigms affords a rigorous and quantitative account of the cognitive mechanisms implicated in drawing inferences from probabilistic feedback. Crucially, within this framework, a weighting factor known as the learning rate

84 controls how the value of unexpected feedback information (also know as the
85 prediction error) is appraised. (20). In experimental settings mimicking real-life,
86 volatile environments, adaptive value-based learning is implemented via a dynamic
87 (that is, time varying) rather than constant learning rate (21-25). Abnormal tuning of
88 the dynamic learning rate distorts processing of probabilistic feedback and impairs
89 learning (26). Prior behavioural evidence suggests that tuning of the dynamic learning
90 rate is disrupted in depression as a function of feedback congruence and valence (27,
91 28).
92
93 In this work, we capitalise on the neural encoding of the dynamic learning rate during
94 probabilistic learning to discriminate response to cCBT. Since successful CBT
95 involves cognitive restructuring of negatively biased thinking we predicted processing
96 of probabilistic negative feedback would uncover between-group differential pre-
97 treatment BOLD activity. Additionally, we found that a learning style that facilitates
98 reframing of negative cognitive biases was associated with response to cCBT.
99
100

METHODS AND MATERIALS

Sample

All 37 participants (18 women) were recruited via self-referral through local newspaper advertisement. Eligibility criteria were a primary diagnosis of depressive disorder as operationalised by ICD-10 diagnostic criteria and a score ≥ 14 on the Beck's Depression Inventory-II (BDI-II). To avoid any potential confound associated with psychotropic medications, we only recruited unmedicated depressed subjects. Exclusion criteria included current involvement with other CBT-based interventions or psychological therapies, a comorbid diagnosis of other major mental disorder, CBT treatment within past 3 years, a diagnosis of psychoactive substance dependence, previous history of brain injury.

Eleven subjects (~29.7%) did not attend the post-treatment assessment. Of these subjects, 6 deteriorated and required treatment with antidepressant medications and 5 did not complete cCBT due to lack of efficacy. High dropout rates are common in studies examining Internet delivered psychotherapies (12). Twenty-six subjects (~70.3%) attended the post-treatment appointment and of these only one was unable to undergo scanning.

In total 19 subjects were classified as responders and 18 subjects were classified as non-responders. The overall cCBT response rate was 51.3%. The average post-treatment improvement in BDI-II score was around 62% (± 40%).

Between-group comparisons revealed no significant differences in age (t_{35}=0.08; p=0.93) and sex (χ^2_1=0.02; p=0.86). Non-responders had a significantly higher pre-

126 treatment BDI-II score than responders (t_{35}=2.86; p=0.006). On further sensitivity
127 analyses we found this significant difference to be mainly determined by those non-
128 responders who did not complete cCBT ($t_{27.3}$=4.74; p<0.001) rather than by those who
129 did (t_{24}=0.62; p=0.53). In spite of these between-group differences in pre-treatment
130 BDI-II scores, we wanted to probe differences in the neurocomputational mechanisms
131 underlying probabilistic learning in order to expose the internal cognitive mechanisms
132 implicated in response to cCBT.
133
134 All participants provided written, informed consent. The study protocol was approved
135 by the West of Scotland Ethics Committee (10/S0703/71).
136
137 ***Experimental design***
138 This study adopted a naturalistic longitudinal design. Participants attended two
139 appointments (pre- and two months post-treatment with cCBT) (see Supplemental
140 Materials for further details on cCBT and study design). Each appointment included a
141 clinical evaluation by a qualified psychiatrist followed by an fMRI scan. A clinical
142 diagnosis of depression was corroborated using the Clinical Interview Schedule –
143 Revised (CIS-R) (29). To measure depression severity we used the BDI-II, which is a
144 clinically-validated tool to assess intensity of depression (30).
145
146 We regarded non-completion of cCBT as an index of treatment failure and classified
147 all non-completers as non-responders. For the remaining subjects response to cCBT
148 was defined as a 50% or greater reduction in the pre-treatment BDI-II score. To
149 account for response bias we performed sensitivity analyses excluding non-
150 completers from the non-responders group.

151

152 ***fMRI experimental paradigm***

153 To probe the neural correlates of probabilistic reinforcement learning we employed a
154 probabilistic reversal-learning task during fMRI (Figure 1). This task involved
155 learning which of two stimuli yielded the highest payoff rate and included 180 trials
156 lasting approximately 20 minutes. Participants were required to choose between two
157 abstract visual stimuli both yielding either positive (+10) or negative (-10) outcome
158 devoid of monetary value. Stimulus-outcome contingencies were probabilistic and
159 asymmetrically skewed (70-30%) (Figure 1).

160

161 Furthermore, to create a volatile environment stimulus-outcome contingencies were
162 reversed in the course of the experiment. Notably, reversals were triggered when
163 participants chose the high probability stimulus (that is, the stimulus with a greater
164 chance of yielding a positive outcome) five times over the last six trials. As a result
165 participants experienced a different number of reversals.

166

167 Participants were advised of the probabilistic nature of the task and that stimulus-
168 outcome contingencies might reverse based upon their performance. Moreover, to
169 ensure participants understood the nature of the task they underwent a 5 minutes
170 practice session prior to the fMRI scan. The task was programmed using
171 Presentation® (Neurobehavioural Systems) stimulus delivery software.

172

173 The probabilistic reversal-learning task is ideally suited to exposing information
174 processing biases during probabilistic learning. Ultimately optimal performance rests
175 upon attaching a greater weight (via a greater learning rate) to more informative

176 *congruent* feedback (that is, feedback that is consistent with the most likely outcome
177 associated with the chosen stimulus) than to less informative *incongruent* feedback
178 (that is, feedback that is not consistent with the most likely outcome associated with
179 the chosen stimulus). To do so subjects need to be able to infer whether fluctuations
180 in observed stimulus-outcome associations reflect either noise (given underlying
181 stochastic contingencies) or sudden environmental changes (that is, reversals).
182
183 In depression there is substantial behavioural evidence that both congruence (27, 28)
184 and the affective quality (i.e. valence) (2) of probabilistic feedback significantly
185 contribute to biasing information processing. Accordingly, in our analyses we
186 leverage the combined effect of congruence and valence on the dynamic learning rate
187 to probe behavioural and neural differences between responders and non-responders.
188
189 ***Behavioural statistical analysis***
190 To verify that individual performance was better than chance we used a binomial test
191 to compare the number of correct choices with chance level.
192
193 To examine for between-group differences in task performance we regressed subject-
194 wise percentage of high probability stimulus choices on clinical outcome after
195 adjusting for pre-treatment BDI-II score. Additionally we tested for any between-
196 group difference in the effect of the high probability stimulus on choice behaviour
197 (the higher the effect of the high probability stimulus the more optimal the choice
198 behaviour and thus learning) using a generalised mixed-effects linear model (see
199 Supplemental Materials for further details on this analysis).
200

Finally we tested for any between-group difference in the model-derived dynamic learning rate estimates as a function of congruence and valence (see Supplemental Materials for further details on this analysis).

Computational modelling of behavioural data

We fitted 5 different models (see Supplementary Materials for further details) that use trial-wise scaling of the prediction error but make different assumptions on the computational mechanisms supporting this dynamic tuning of learning rate.

In the winning model the learning rate scales with the slope of the smoothed unsigned prediction error (i.e. absolute value of prediction error) (24). This model reprises Pearce-Hall's theory that surprise (formalised as the unsigned prediction error) drives the acquisition of stochastic stimulus-outcome contingencies (31) but with some important refinements. Indeed, compared to the Pearce-Hall's model, the smoothing of the unsigned prediction error (the degree of which is regulated by a free parameter ρ) should render the inference process about whether a change has occurred in the environment more robust to the inherent task stochasticity. Moreover, an additional free parameter γ controls the extent to which the dynamic updating of the learning rate is influenced by the slope. For example, whilst lower values of γ yield substantial trial-by-trial changes of the dynamic learning rate even in the presence of small slope estimates (that is, low surprise), higher values of γ result in a more stable learning rate even in the presence of significant slope estimates (that is, high surprise). Hence, this model also allows for the possibility that subjects might be employing a relatively fixed learning rate. The decision function for all models was a

standard sigmoid function parameterised by the inverse of the temperature parameter, β.

Model fitting and model comparison

To optimise each model's free parameters we implemented the hierarchical type II maximum likelihood fitting procedure described in (32) (see Supplemental Materials for further details). The fits of all models were compared using the Integrated Bayesian Information Criterion (BIC_{int}) (32) (see Supplemental Materials for further details).

To ascertain any between-group differences in the learning style encoded in the model's fixed parameters we regressed subject-wise parameter estimates against clinical outcome (response vs. non-response) after adjusting for pre-treatment BDI-II score. To account for the response bias we performed additional sensitivity analyses.

Finally we ran sanity checks on the winning model's goodness of fit. To verify accuracy of model's fit we first binned predicted choice propensities according to their quintiles and subsequently measured the strength of their linear association with corresponding observed choice probabilities using Pearson's correlation coefficient. Additionally, we employed a binomial test to test whether the number of choices correctly predicted by the model exceeded that expected by chance (33).

fMRI data acquisition

We used a 3T GE system with an 8-channel parallel imaging head coil. We acquired a high-resolution T_1- weighted structural image (0.5 x 0.5 x 1 mm voxels, 320 x 320

matrix, 160 axial slices, TI = 500 ms, TR = 7700 ms, TE = 1.5 ms, flip angle = 12^{o}) using an optimized Inversion Recovery Fast SPoiled GRadient echo sequence (IR-FSPGR) and a functional echo planar imaging (EPI) scan (3 mm isotropic voxels, 64 x 64 matrix, 608 axial slices, TR = 2000 ms, TE = 30 ms, flip angle = 80^{o}). Slice orientation was tilted -20^{o} from the AC-PC plane to alleviate signal drop out in the orbitofrontal cortex (34). The first four volumes of the functional scan were discarded in order to allow for the magnetic field to reach the steady state.

fMRI data preprocessing and statistical analysis

Pre-treatment and post-treatment fMRI data preprocessing and statistical analyses were performed using FSL software (35). Preprocessing pipeline involved intra-modal motion correction using MCFLIRT (36), slice timing correction, spatial smoothing with an isotropic 5 mm FWHM Gaussian kernel, high-pass temporal filtering with 110 sec. cut-off frequency and grand-mean intensity normalisation of each entire 4D dataset. Functional scans were subsequently co-registered with skull-stripped structural images using boundary-based registration (FLIRT) (37, 38) and spatially normalised into MNI152 space using FNIRT non-linear registration.

Whole brain statistical analyses of pre-treatment fMRI data were performed using a multilevel mixed-effects approach as implemented in FLAME1 (FSL) (39). At the first-level the subject-specific general linear model included the model-derived dynamic learning rate as the regressor of interest plus a number of additional nuisance covariates (see Supplementary Materials for further details). Most importantly, we included a nuisance regressor accounting for surprise (here formalised as unsigned

prediction error) to retrieve the unique effect of the dynamic learning rate on BOLD activity.

To improve efficiency of our fMRI statistical analysis all model-derived regressors were obtained by generating subject-wise model fits using the population-level parameter means (40). All regressors were convolved with a hemodynamic response function (double gamma function).

We estimated the subject-wise linear contrasts of parameter estimates and subsequently entered these contrast images into a second-level mixed-effects analysis where we tested both mean group effect and between-group (responders vs. non-responders) differences. We thresholded the resulting Z statistic images using cluster-defining threshold of $Z>3.1$ and a FWE-corrected significance threshold of $p=0.05$.

Furthermore, we examined for any between-group difference in the pre-treatment BOLD activity encoding the dynamic learning rate. To this end we first retrieved BOLD percent signal change time-locked to the onset of the outcome phase from a cluster broadly corresponding to the dmPFC (max $Z=7.25$; -4 -2 56). We chose this cluster since it is consistent with previous reports on the fMRI correlates of the dynamic learning rate (24, 41). Subsequently we performed between-group comparisons as a function of feedback congruence and valence using mixed-effects linear models (see Supplemental Materials for further details on this analysis).

297 We also assessed for a robust linear association between subject-wise (that is,
298 aggregated up to the subject-level) pre-treatment event-locked BOLD percent signal
299 change and post-treatment symptomatic improvement.
300
301 Having ascertained between-group differences in pre-treatment BOLD activity we
302 sought to determine whether such BOLD activity was either a moderator or mediator
303 of cCBT response. (see Supplemental Materials for further details on this analysis).
304
305

RESULTS

Clinical outcome

Between-group comparisons revealed no significant differences in age (t_{35}=0.08; p=0.93) and sex (χ^2_1=0.02; p=0.86) between responders and non-responders. Non-responders had a significantly higher pre-treatment BDI-II score than responders (t_{35}=2.86; p=0.006). On further sensitivity analyses we found this significant difference to be mainly determined by those non-responders who did not complete cCBT ($t_{27.3}$=4.74; p<0.001) rather than by those who did (t_{24}=0.62; p=0.53). In spite of these between-group differences in pre-treatment BDI-II scores, we wanted to probe differences in the neurocomputational mechanisms underlying probabilistic learning in order to expose the internal cognitive mechanisms implicated in response to cCBT.

Task performance and behavioural estimates of the dynamic learning rate do not discriminate response to cCBT

All participants did not choose randomly (binomial test, mu=0.5, p<0.05) during the task. We did not find any significant between-group difference in the number of buffer trials (t_{35}=-0.41; p=0.68) during the pre-treatment experiment. Task performance was similar across responders and non-responders (see Supplemental Results for further details).

Pre-treatment behavioural estimates of the dynamic learning rate as a function of congruence and valence did not discriminate between responders and non-responders (congruent positive: $t_{38.77}$=-0.24, p=0.80; incongruent positive: $t_{37.2}$=0.45, p=0.65;

330 congruent negative: $t_{38.07}$=0.30, p=0.76; incongruent negative: $t_{159.97}$=-0.41, p=0.67)
331 (Figure 2).
332
333 ***Model comparison***
334 On formal Bayesian model comparison we found that the best fitting model was that
335 described in (24) with a BIC_{int} of ~287 (32). (Krugel et al. model with additional
336 parameter α^1: BIC_{int}=540.82; Hierarchical Gaussian Filter: BIC_{int}=828.68; Pearce-
337 Hall: BIC_{int}=332.72; Kalman filter K1 variant: BIC_{int}=708.70) (Figure 3A).
338
339 We verified the model's goodness of fit using a binomial test and found that under the
340 null hypothesis that on each trial the model was choosing at chance level, the
341 probability of model's correctly predicted *n* choices was <0.05 across all subjects.
342 Additionally we found that observed and model's predicted choice probabilities were
343 significantly correlated (r = 0.88; p<0.001), further endorsing the quality of the model
344 fits (Figure 3B).
345
346 ***Parameters reflecting specific information processing style are associated***
347 ***with differential response to cCBT***
348 After adjusting for pre-treatment BDI-II score, we found a statistically significant
349 between-group difference in the estimates of the model's parameter ρ (logit(ρ): t_{34}=-
350 2.15; p=0.038) and γ (log(γ): t_{34}=2.11; p=0.041) (Figure 4) but no significant
351 difference for β (log(β): t_{34}=0.61; p=0.54). Additional sensitivity analyses revealed
352 these significant differences to be predominantly driven by non-responders who did
353 not complete cCBT (logit(ρ): t_{27}=-3.12; p=0.004; log(γ): t_{27}=2.99; p=0.005) rather
354 than by those who did (logit(ρ): t_{23}=-0.72; p=0.47; log(γ): t_{23}=0.65; p=0.51).

In sum, responders were on average more prone (that is, lower mean estimate of ρ) to smoothing over previous unsigned prediction errors than non-responders. This implies that responders took greater account of previous feedback history than non-responders. Additionally, on average responders had a tendency to make relatively smaller trial-wise adjustments of the learning rate (that is, greater mean estimate of γ) as a result of outcome surprisingness than non-responders.

Neural signature of dynamic learning rate

Whole-brain model-based fMRI analysis of pre-treatment fMRI data revealed significant bilateral activations correlating with the dynamic learning rate in a set of brain regions broadly located in the dorsomedial prefrontal cortex (dmPFC), dorsolateral prefrontal cortex (including precentral gyrus, postcentral gyrus) and occipital cortex (fusiform gyrus, lingual gyrus) (Supplemental Table S1). Significant activations survived family-wise error (FWE) correction for multiple comparisons ($p < 0.05$) at the cluster level with a cluster-defining threshold of $p < 0.001$.

A number of previous studies have suggested that the dmPFC in particular might be involved in the dynamic online adjusting of the learning rate (22, 41, 42), although they employed different samples, experimental paradigms and modelling assumptions. Moreover, previous work reported abnormal activation of this region in response to probabilistic feedback in a sample of unmedicated depressed subjects compared to healthy controls (28). We therefore used BOLD activity in the bilateral dmPFC shown in Figure 5 to discriminate treatment response (see Materials and Methods for further details).

380

381 ***Pre-treatment BOLD activity encoding dynamic learning rate discriminates***

382 ***between responders and non-responders***

383 A two-sample unpaired t-test on the dynamic learning rate contrast images did not
384 identify any significant between group differences. However, on between-group
385 comparisons of the outcome-locked BOLD activity in the dmPFC we found that
386 responders exhibited significantly greater BOLD percent signal change during
387 incongruent negative trials ($F_{1,34.07}$=8.87, p=0.005) and significantly lower BOLD
388 percent signal change during congruent negative trials ($F_{1,33.01}$=5.15, p=0.029)
389 compared to non-responders (Figure 6). No significant between-group differences
390 were found following positive feedback (congruent: $F_{1,34.72}$=1.45, p=0.23;
391 incongruent: $F_{1,33.79}$=0.33, p=0.56) (Figure 6).

392

393 Without non-completers between-group differences remained significant only during
394 incongruent negative trials ($F_{1,23.18}$=4.99, p=0.03). No significant difference was
395 detected regarding congruent negative feedback ($F_{1,23.02}$=1.23, p=0.27) (Supplemental
396 Figure S1). Moreover, we found a statistically significant negative correlation
397 between treatment response magnitude and BOLD activity in incongruent negative
398 trials (t_{24}=-3.87, p<0.001) but not in congruent negative trials (t_{24}=0.36, p=0.72)
399 (Figure 7).

400

401

DISCUSSION

In the present study, to discriminate response to cCBT in depression we examined pre-treatment BOLD activity correlating with dynamic appraisal of probabilistic feedback during reinforcement learning. We found that greater BOLD activity in the dmPFC during incongruent negative trials and lower BOLD activity during congruent negative trials were associated with response to cCBT. Furthermore, we provided preliminary evidence that this pattern of BOLD activity may be moderating, rather than mediating, the effect of cCBT on clinical outcome (see Supplemental Results).

Crucially, although the focus of CBT in depression is centred in fostering adaptive reappraisal strategies (43), to the best of our knowledge no previous study has examined processing of probabilistic feedback as a function of response to CBT. Moreover, in spite of converging evidence that behavioural and neural responses to probabilistic feedback are abnormal in depression, the cognitive mechanisms underlying such impairment are still unknown and relatively unexplored. In this study we have addressed this knowledge gap by explicitly modelling the neurocomputational mechanisms of inference implicated in probabilistic reinforcement learning as a function of treatment response.

At a computational level we have capitalised on the notion that the model's optimised fixed parameters capture a person's typical mode of appraising incoming probabilistic information. We found that responders took greater account of previous feedback history than non-responders by means of greater smoothing over previous unsigned prediction errors. This operation helps averaging out noisy feedback from the trial-by-trial online computation of surprise and therefore makes inference more robust to

427 random noisy fluctuations in the statistics of the environment. Somewhat
428 complementary to this finding we found that responders were inclined to make
429 smaller adjustments to the learning rate as a result of surprising outcomes. Again, this
430 feature confers a relatively greater degree of robustness against noise to the inference
431 process as it makes the temporal trajectory of the learning rate more stable.
432
433 On the whole, this specific information processing style fosters comparatively more
434 farsighted and judicious decision-making in the responders group. CBT helps patients
435 reframe extreme and dysfunctional negative thoughts in a more considered and
436 balanced fashion (44). One fundamental requirement for CBT to be effective is the
437 patient's ability to actively engage in such work of cognitive restructuring. Depressed
438 patients who are more adept at thoughtfully sieving through the barrage of noisy
439 feedback information surrounding them exhibit a greater predisposition to critical
440 thinking. This may translate in a greater ability to challenge maladaptive thinking
441 patterns. Consistent with this line of reasoning is the prior finding that pre-treatment
442 clinical ratings indicative of lower dysfunctional attitudes (as a result of less rigid and
443 extreme thinking) predict better response to cCBT (12).
444
445 At the behavioural and neural level we have probed between-group differences in the
446 online inference process underlying probabilistic learning, here quantified by a
447 dynamic learning rate. Behaviourally model's derived estimates of the dynamic
448 learning rate did not discriminate response to cCBT. In contrast, BOLD activity did.
449 Significant imaging but not behavioural results are not uncommon in cognitive
450 neuroscience (45). One possible explanation is that underlying between-group
451 differences are better captured by measures of neural activity. Additionally, lack of

452 behavioural corroboration in our study may be due to the specific modelling approach
453 employed here or simply to inadequate power. Crucially, our finding that neural, and
454 not behavioural, measures of information processing discriminate response to cCBT
455 underscores the translational potential of neuroimaging biomarkers in treatment
456 prediction research in psychiatry.
457
458 We have shown that BOLD activity in the dmPFC underpins online appraisal of
459 probabilistic feedback. Our cluster in the dmPFC largely overlaps with the anterior
460 mid-cingulate cortex (aMCC). In a recent review of the functional roles ascribed to
461 the aMCC Shackman et al. proposed that the core function of this region is to
462 determine optimal choice behaviour under conditions of uncertainty (46). During
463 probabilistic learning the differential evaluation of noisy and stochastic feedback is
464 the main mechanism by which an agent tackles environmental uncertainty in the
465 service of adaptive instrumental behaviour. In the computational framework
466 employed here the dynamic learning rate encodes this flexible trial-wise weighting of
467 information. Thus, our finding fits in with current theoretical accounts regarding the
468 involvement of the aMCC in uncertainty resolution (46, 47).
469
470 In particular, we have shown that BOLD activity in the dmPFC denotes a tendency to
471 assign comparatively smaller weight to negative, although still informative, feedback
472 amongst responders. This may be symptomatic of a comparatively greater ability to
473 maintain a positive outlook in spite of adverse events as the expected value of adverse
474 events is more likely to be underestimated (48). Ultimately, a relatively greater
475 capacity to lessen the detrimental impact that day-to-day setbacks can have on one's

476 own view of himself and the surrounding world may facilitate reframing of unhelpful
477 thoughts and help boost response to CBT.
478
479 In contrast, during incongruent negative trials, BOLD activity in the dmPFC speaks to
480 a relatively greater propensity to encode negative but less accurate feedback in the
481 responders group and is thus expected to bias behavioural responses away from
482 advantageous choices. Notably, this finding was robust to response bias and was
483 further corroborated by a significant negative correlation between BOLD activity and
484 post-treatment symptomatic improvement. Interestingly, our results concord with a
485 previous report by Taylor Tavares et al. that lower BOLD activity in the dmPFC was
486 associated with failure to disregard incongruent negative feedback (28).
487
488 At first glance, it would seem counterintuitive for such a pattern of pre-treatment
489 BOLD activity to be associated with clinical improvement. Relatively greater
490 underestimation of the value of generally advantageous choices may cause lack of
491 engagement with positive states and ultimately engender an unduly negative view of
492 the self and the world. One obvious interpretation is that this pattern of BOLD activity
493 is the therapeutic target of CBT. However, this hypothesis is called into question by
494 the observation that cross-session BOLD activity does not change within the
495 responders group (see Supplemental Results). An alternative explanation is that a
496 comparatively greater underestimation of advantageous choices serves the purpose of
497 dampening down expectations on the amount of positive feedback that can be derived
498 from those choices. This may render responders relatively more immune to the
499 disappointment of high expectations not being met and thus buffer the deleterious

consequences that negative, although somewhat misleading, events may have on mood.

In conclusion, in this study we have provided evidence supporting utility and feasibility of a neurocomputational approach to treatment response prediction in depression and, more in general, in mental health research. In particular, we have shown that computational and neural correlates of probabilistic reinforcement learning enable early discrimination of treatment response to cCBT in depression.

ACKNOWLEDGEMENTS

The authors are grateful to Dr Rajeev Krishnadas for helpful discussion on the study, Dr John McLean for expert technical support and Prof Chris Williams for his help with the CBT-based intervention (http://llttf.com).

This work was supported by a Chief Scientist Office grant (PN09CP214) and the Dr Mortimer and Theresa Sackler Foundation. F.Q. is supported by an MRC- and MRF-funded clinical research training fellowship (PsySTAR). E.F. and M.G.P were supported by the Biotechnology and Biological Sciences Research Council (BBSRC; grant BB/J015393/2 to M.G.P.) and the Economic and Social Research Council (ESRC; grant ES/L012995/1 to M.G.P.).

FINANCIAL DISCLOSURE

The authors have neither conflicts of interest nor financial interests to declare.

REFERENCES

1. Beck AT (1972): *Depression; causes and treatment*. Philadelphia,: University of Pennsylvania Press.

2. Eshel N, Roiser JP (2010): Reward and punishment processing in depression. *Biological psychiatry*. 68:118-124.

3. Beck AT (1976): *Cognitive therapy and the emotional disorders*. New York: International Universities Press.

4. Cuijpers P, Berking M, Andersson G, Quigley L, Kleiboer A, Dobson KS (2013): A meta-analysis of cognitive-behavioural therapy for adult depression, alone and in comparison with other treatments. *Can J Psychiatry*. 58:376-385.

5. Cuijpers P, Donker T, Johansson R, Mohr DC, van Straten A, Andersson G (2011): Self-guided psychological treatment for depressive symptoms: a meta-analysis. *PloS one*. 6:e21274.

6. Siegle GJ, Thompson WK, Collier A, Berman SR, Feldmiller J, Thase ME, et al. (2012): Toward clinically useful neuroimaging in depression treatment: prognostic utility of subgenual cingulate activity for determining depression outcome in cognitive therapy across studies, scanners, and patient characteristics. *Arch Gen Psychiatry*. 69:913-924.

7. Siegle GJ, Carter CS, Thase ME (2006): Use of FMRI to predict recovery from unipolar depression with cognitive behavior therapy. *The American journal of psychiatry*. 163:735-738.

8. McGrath CL, Kelley ME, Holtzheimer PE, Dunlop BW, Craighead WE, Franco AR, et al. (2013): Toward a neuroimaging treatment selection biomarker for major depressive disorder. *JAMA Psychiatry*. 70:821-829.

548 9. Button KS, Wiles NJ, Lewis G, Peters TJ, Kessler D (2012): Factors
549 associated with differential response to online cognitive behavioural therapy. *Soc*
550 *Psychiatry Psychiatr Epidemiol*. 47:827-833.
551 10. Spek V, Nyklicek I, Cuijpers P, Pop V (2008): Predictors of outcome of group
552 and internet-based cognitive behavior therapy. *J Affect Disord*. 105:137-145.
553 11. de Graaf LE, Hollon SD, Huibers MJ (2010): Predicting outcome in
554 computerized cognitive behavioral therapy for depression in primary care: A
555 randomized trial. *J Consult Clin Psychol*. 78:184-189.
556 12. Donker T, Batterham PJ, Warmerdam L, Bennett K, Bennett A, Cuijpers P, et
557 al. (2013): Predictors and moderators of response to internet-delivered Interpersonal
558 Psychotherapy and Cognitive Behavior Therapy for depression. *J Affect Disord*.
559 151:343-351.
560 13. Thase ME (2014): Using biomarkers to predict treatment response in major
561 depressive disorder: evidence from past and present studies. *Dialogues in clinical*
562 *neuroscience*. 16:539-544.
563 14. Kapur S, Phillips AG, Insel TR (2012): Why has it taken so long for biological
564 psychiatry to develop clinical tests and what to do about it? *Molecular psychiatry*.
565 17:1174-1179.
566 15. DeRubeis RJ, Siegle GJ, Hollon SD (2008): Cognitive therapy versus
567 medication for depression: treatment outcomes and neural mechanisms. *Nat Rev*
568 *Neurosci*. 9:788-796.
569 16. Ritchey M, Dolcos F, Eddington KM, Strauman TJ, Cabeza R (2011): Neural
570 correlates of emotional processing in depression: changes with cognitive behavioral
571 therapy and predictors of treatment response. *J Psychiatr Res*. 45:577-587.

572 17. Siegle GJ, Thompson W, Carter CS, Steinhauer SR, Thase ME (2007):
573 Increased amygdala and decreased dorsolateral prefrontal BOLD responses in
574 unipolar depression: related and independent features. *Biological psychiatry*. 61:198-
575 209.
576 18. Goldapple K, Segal Z, Garson C, Lau M, Bieling P, Kennedy S, et al. (2004):
577 Modulation of cortical-limbic pathways in major depression: treatment-specific
578 effects of cognitive behavior therapy. *Arch Gen Psychiatry*. 61:34-41.
579 19. McGrath CL, Kelley ME, Dunlop BW, Holtzheimer PE, 3rd, Craighead WE,
580 Mayberg HS (2014): Pretreatment brain states identify likely nonresponse to standard
581 treatments for depression. *Biological psychiatry*. 76:527-535.
582 20. Maia TV (2009): Reinforcement learning, conditioning, and the brain:
583 Successes and challenges. *Cogn Affect Behav Neurosci*. 9:343-364.
584 21. Payzan-LeNestour E, Bossaerts P (2011): Risk, unexpected uncertainty, and
585 estimation uncertainty: Bayesian learning in unstable settings. *PLoS Comput Biol*.
586 7:e1001048.
587 22. Behrens TE, Woolrich MW, Walton ME, Rushworth MF (2007): Learning the
588 value of information in an uncertain world. *Nat Neurosci*. 10:1214-1221.
589 23. Nassar MR, Wilson RC, Heasly B, Gold JI (2010): An approximately
590 Bayesian delta-rule model explains the dynamics of belief updating in a changing
591 environment. *The Journal of neuroscience : the official journal of the Society for*
592 *Neuroscience*. 30:12366-12378.
593 24. Krugel LK, Biele G, Mohr PN, Li SC, Heekeren HR (2009): Genetic variation
594 in dopaminergic neuromodulation influences the ability to rapidly and flexibly adapt
595 decisions. *Proceedings of the National Academy of Sciences of the United States of*
596 *America*. 106:17951-17956.

597 25. Mathys C, Daunizeau J, Friston KJ, Stephan KE (2011): A bayesian
598 foundation for individual learning under uncertainty. *Front Hum Neurosci*. 5:39.
599 26. Browning M, Behrens TE, Jocham G, O'Reilly JX, Bishop SJ (2015): Anxious
600 individuals have difficulty learning the causal statistics of aversive environments. *Nat*
601 *Neurosci*. 18:590-596.
602 27. Murphy FC, Michael A, Robbins TW, Sahakian BJ (2003):
603 Neuropsychological impairment in patients with major depressive disorder: the effects
604 of feedback on task performance. *Psychol Med*. 33:455-467.
605 28. Taylor Tavares JV, Clark L, Furey ML, Williams GB, Sahakian BJ, Drevets
606 WC (2008): Neural basis of abnormal response to negative feedback in unmedicated
607 mood disorders. *NeuroImage*. 42:1118-1126.
608 29. Lewis G, Pelosi AJ, Araya R, Dunn G (1992): Measuring psychiatric disorder
609 in the community: a standardized assessment for use by lay interviewers. *Psychol*
610 *Med*. 22:465-486.
611 30. Beck AT, Steer RA, Ball R, Ranieri W (1996): Comparison of Beck
612 Depression Inventories -IA and -II in psychiatric outpatients. *J Pers Assess*. 67:588-
613 597.
614 31. Pearce JM, Hall G (1980): A model for Pavlovian learning: variations in the
615 effectiveness of conditioned but not of unconditioned stimuli. *Psychol Rev*. 87:532-
616 552.
617 32. Huys QJ, Eshel N, O'Nions E, Sheridan L, Dayan P, Roiser JP (2012): Bonsai
618 trees in your head: how the pavlovian system sculpts goal-directed choices by pruning
619 decision trees. *PLoS Comput Biol*. 8:e1002410.

620 33. Huys QJ, Cools R, Golzer M, Friedel E, Heinz A, Dolan RJ, et al. (2011):
621 Disentangling the roles of approach, activation and valence in instrumental and
622 pavlovian responding. *PLoS Comput Biol*. 7:e1002028.
623 34. Deichmann R, Gottfried JA, Hutton C, Turner R (2003): Optimized EPI for
624 fMRI studies of the orbitofrontal cortex. *NeuroImage*. 19:430-441.
625 35. Smith SM, Jenkinson M, Woolrich MW, Beckmann CF, Behrens TE,
626 Johansen-Berg H, et al. (2004): Advances in functional and structural MR image
627 analysis and implementation as FSL. *NeuroImage*. 23 Suppl 1:S208-219.
628 36. Jenkinson M, Bannister P, Brady M, Smith S (2002): Improved optimization
629 for the robust and accurate linear registration and motion correction of brain images.
630 *NeuroImage*. 17:825-841.
631 37. Jenkinson M, Smith S (2001): A global optimisation method for robust affine
632 registration of brain images. *Medical image analysis*. 5:143-156.
633 38. Greve DN, Fischl B (2009): Accurate and robust brain image alignment using
634 boundary-based registration. *NeuroImage*. 48:63-72.
635 39. Beckmann CF, Jenkinson M, Smith SM (2003): General multilevel linear
636 modeling for group analysis in FMRI. *NeuroImage*. 20:1052-1063.
637 40. Daw ND, O'Doherty JP, Dayan P, Seymour B, Dolan RJ (2006): Cortical
638 substrates for exploratory decisions in humans. *Nature*. 441:876-879.
639 41. Iglesias S, Mathys C, Brodersen KH, Kasper L, Piccirelli M, den Ouden HE,
640 et al. (2013): Hierarchical prediction errors in midbrain and basal forebrain during
641 sensory learning. *Neuron*. 80:519-530.
642 42. McGuire JT, Nassar MR, Gold JI, Kable JW (2014): Functionally dissociable
643 influences on learning rate in a dynamic environment. *Neuron*. 84:870-881.
644 43. Beck AT (1979): *Cognitive therapy of depression*. New York: Guilford Press.

645 44. Wright JH, Beck AT (1983): Cognitive Therapy of Depression - Theory and
646 Practice. *Hosp Community Psych*. 34:1119-1127.
647 45. Wilkinson D, Halligan P (2004): The relevance of behavioural measures for
648 functional-imaging studies of cognition. *Nat Rev Neurosci*. 5:67-73.
649 46. Shackman AJ, Salomons TV, Slagter HA, Fox AS, Winter JJ, Davidson RJ
650 (2011): The integration of negative affect, pain and cognitive control in the cingulate
651 cortex. *Nat Rev Neurosci*. 12:154-167.
652 47. Rushworth MF, Behrens TE (2008): Choice, uncertainty and value in
653 prefrontal and cingulate cortex. *Nat Neurosci*. 11:389-397.
654 48. Sharot T (2011): The optimism bias. *Time*. 177:40-44, 46.
655 49. Wager TD, Nichols TE (2003): Optimization of experimental design in fMRI:
656 a general framework using a genetic algorithm. *NeuroImage*. 18:293-309.
657
658

FIGURE LEGENDS

Figure 1. Probabilistic reversal-learning task.

(A) Each trial commenced with a jittered interstimulus interval (1-4s) displaying a fixation cross. Subsequent to this two abstract visual stimuli appeared randomly on either side of the screen for 1.25s. For each participant the two stimuli were randomly chosen from a pool of 18 different geometrical shapes. Participants were given 1s to choose a stimulus via a button press. Following a second jittered interstimulus interval (1-4s) participants were presented with the outcome of their decision for 0.65s. Outcome was either positive (+10) or negative (-10). To maximize design efficiency the duration of jittered interstimulus intervals was optimized implementing a genetic algorithm described in (49). ISI: Interstimulus Interval.

(B) Classification of probabilistic feedback as a function of congruence and valence. Stimulus-outcome contingencies were asymmetrically skewed (70-30%) so that the expected value of the two stimuli was of the same magnitude but of opposite sign. This meant that whilst one stimulus (here referred to as the high probability stimulus) was associated with a greater likelihood of positive outcome, the other stimulus (here referred to as the low probability stimulus) was associated with a greater likelihood of negative outcome. Reversals were self-paced and occurred when participants chose the high probability stimulus five times over the last six trials. To prevent participants from figuring out the underlying reversal rule we ran a randomly generated number of buffer trials from a zero-truncated Poisson distribution before reversing stimulus-outcome contingencies. The stimulus-outcome association strength was chosen to enable detection of reversals. Participants were only advised of the probabilistic nature of the task and that

684 stimulus-outcome contingencies might reverse based upon their performance.

685 HPS: High Probability Stimulus. LPS: Low Probability Stimulus.

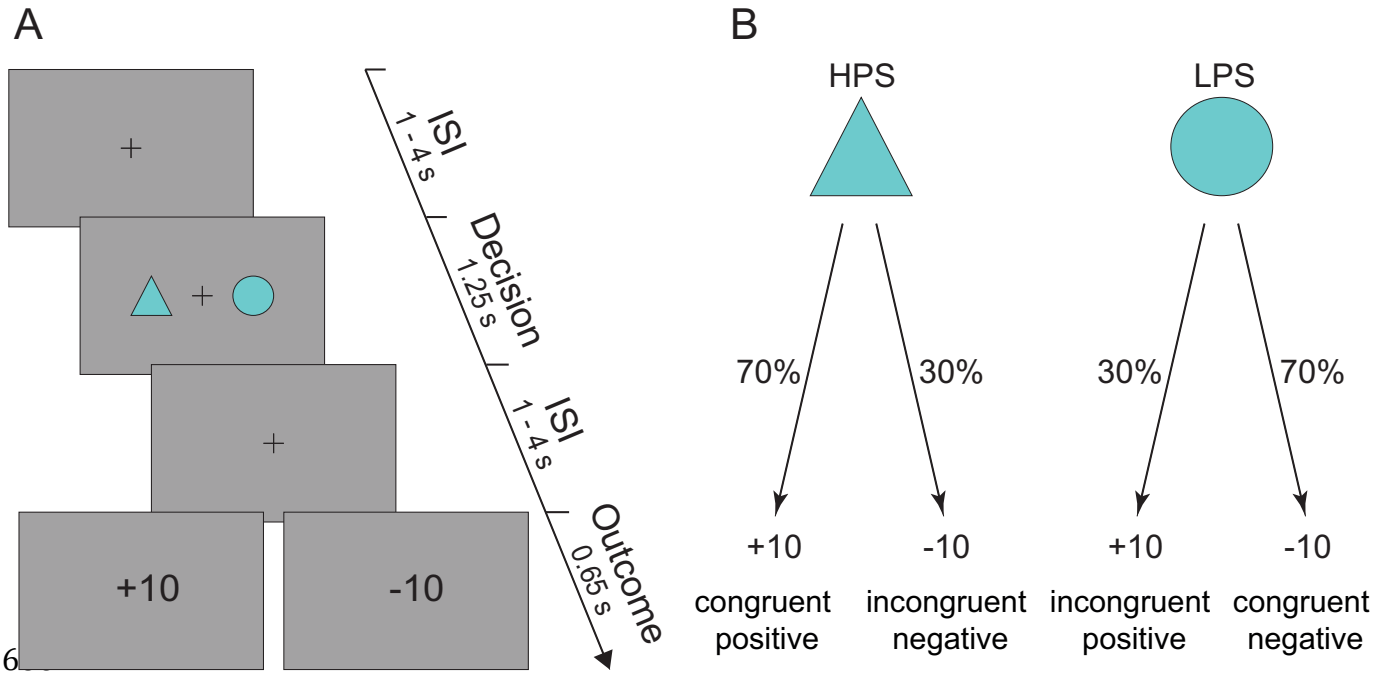

687

688 **Figure 2. Analysis of behavioural estimates of dynamic learning rate.**

689 Least-square mean estimates ± SEM (error bars) of dynamic learning rate in the
690 responders (blue; n=19) and non-responders (red; n=18) groups are plotted as a
691 function of feedback congruence and valence. None of the post-hoc between-group
692 comparisons were statistically significant.

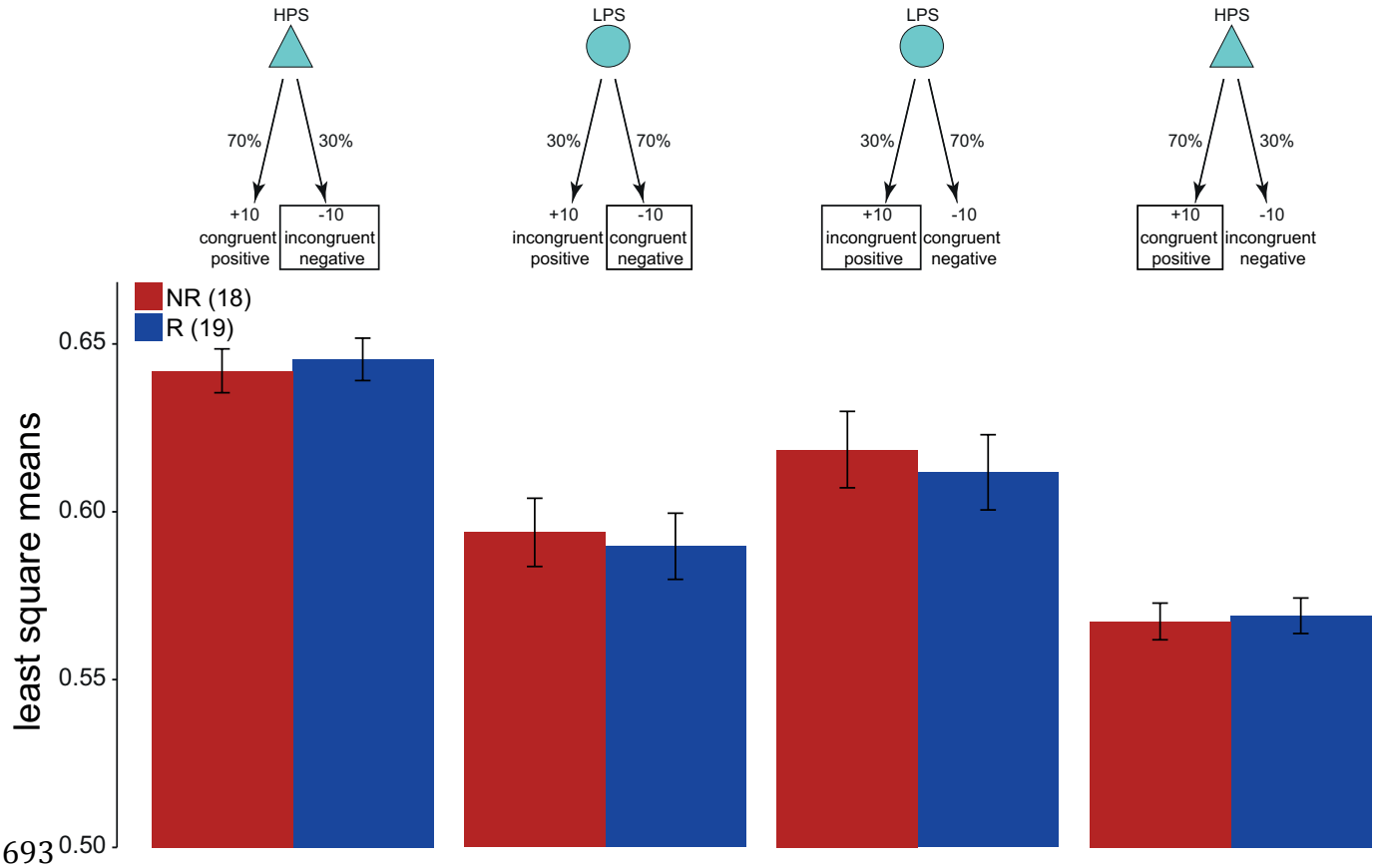

693

694

Figure 3. Computational model comparison and behavioural fit.

(A) BIC_{Int} scores for all models. Lower scores indicate better fit. DYNA is the winning model. DYNA: Krugel et al.'s model. $DYNA_0$: Krugel et al.'s model with additional parameter α^1. HGF: Hierarchical Gaussian Filter. P-H: Pearce-Hall. K1: Kalman filter K1 variant.

(B) Scatterplot shows linear relationship between empirical and predicted choice probabilities. r: Pearson's correlation coefficient.

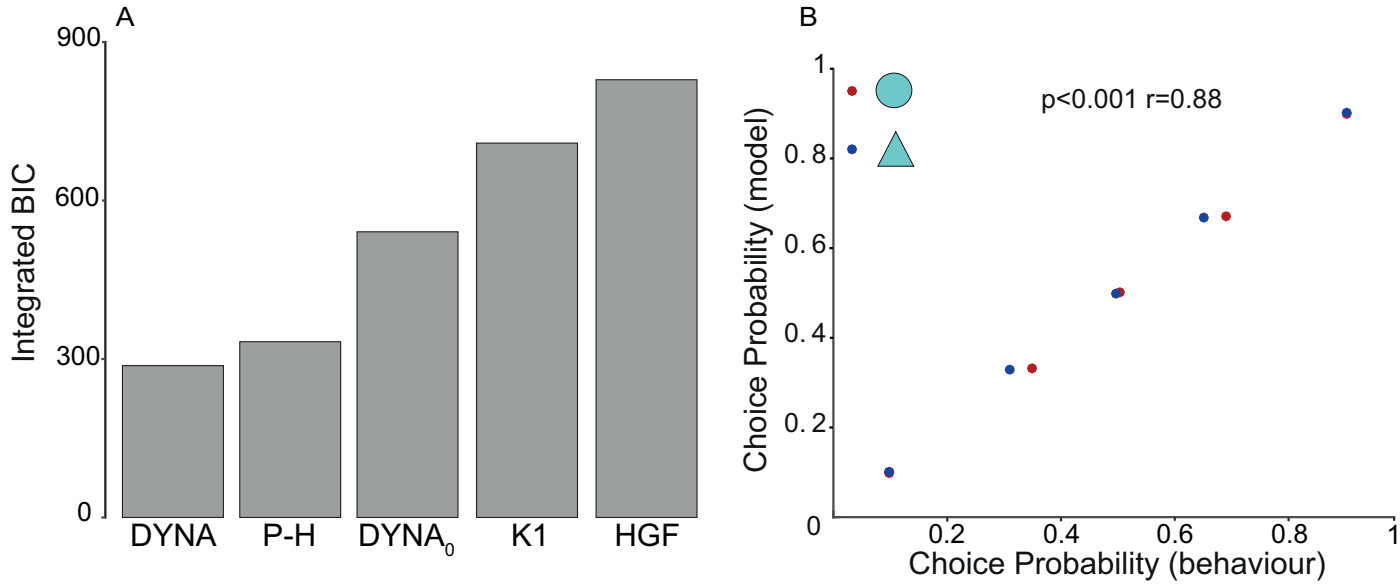

Figure 4. Computational parameters.

Mean estimates ± SEM (error bars) of ρ (left) and γ (right) in the responders (blue) and non-responders (red) groups. Parameter estimates are shown in their native space (logit for ρ and log for γ). After adjusting for pre-treatment BDI-II score, on average responders exhibited a greater tendency to smooth over previous unsigned prediction errors (lower ρ mean estimate) and to make smaller adjustments to the dynamic learning rate (greater γ mean estimate) compared to non-responders. Black circles represent individual subjects. * $p < 0.05$.

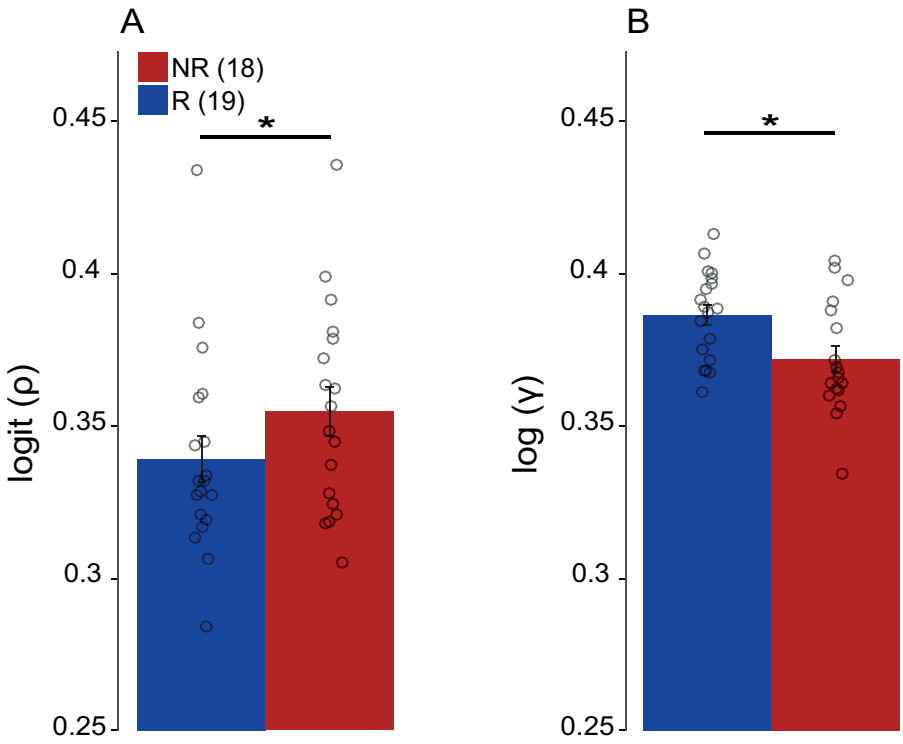

Figure 5. Pre-treatment whole-brain results for dynamic learning rate contrast.

Activations shown here survived a cluster-defining threshold of Z > 3.1 and FWE-corrected significance threshold of p = 0.05. (A) dmPFC: dorsomedial prefrontal cortex. (B) IC: intracalcarine cortex (C) dlPFC: dorsolateral prefrontal cortex. Coordinates are given in the MNI space. We used the cluster in the dmPFC to extract trial-wise feedback-locked BOLD percent signal change for all participants and used them to discriminate treatment response.

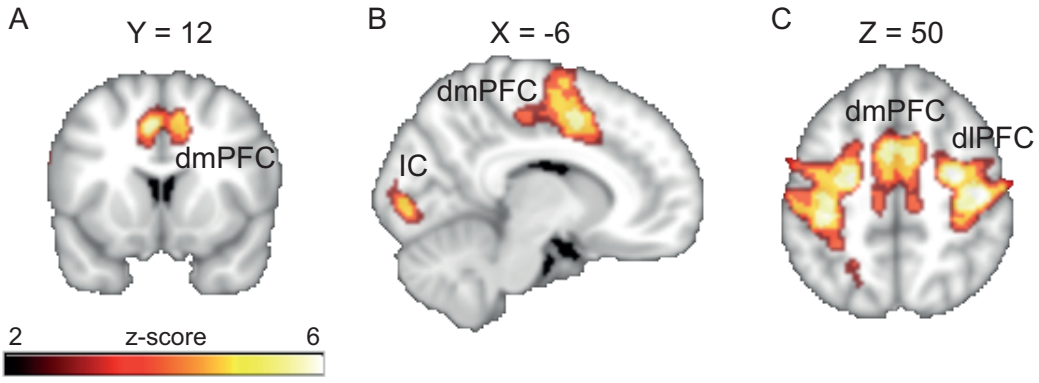

Figure 6. Pre-treatment time course of BOLD percent signal change in the dmPFC.

Average feedback-locked BOLD percent signal change ± SEM (blue and red shading) in responders (blue; n=19) and non-responders (red; n=18) groups is plotted as a function of feedback valence and congruence. Averages are adjusted for pre-treatment BDI-II score. We performed between-group comparisons over the temporal window shown by the grey shaded box. Responders exhibited comparatively lower BOLD activity during congruent negative trials (bottom left; F(1,33.01)=5.15, p=0.029) but comparatively higher BOLD activity during incongruent negative trials (bottom right; F(1,34.07)=8.87, p=0.005).

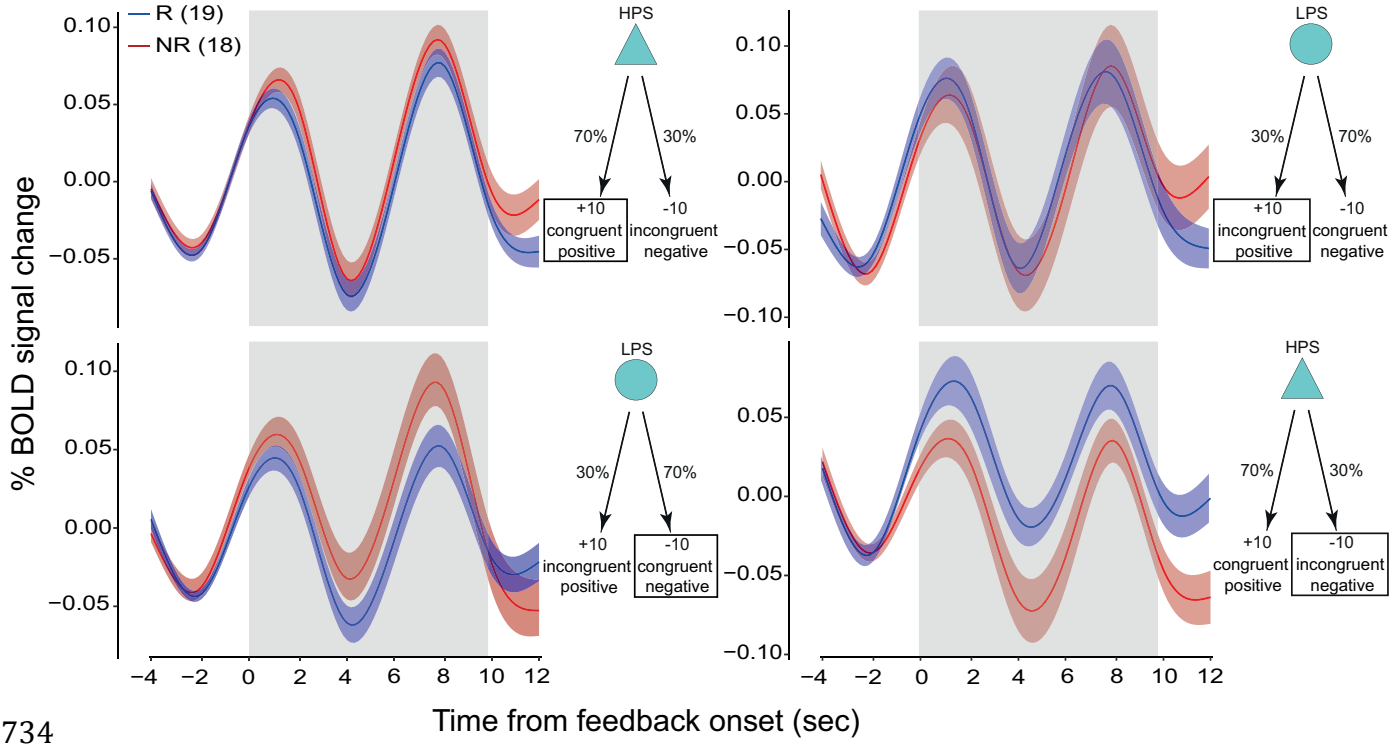

736 **Figure 7. Relationship between BOLD percent signal change in the**
737 **dmPFC and treatment response.**

738 Scatterplots show robust linear fit ± 95% CI (grey shading) of adjusted post-treatment
739 BDI-II score against pre-treatment BOLD percent signal change in the dmPFC. Left:
740 Congruent negative trials. Right: Incongruent negative trials. Post-treatment BDI-II
741 score is adjusted for pre-treatment BDI-II score. Subject-wise pre-treatment BOLD
742 percent signal change is averaged over a time window extending from 4 to 6 seconds
743 after the onset of the outcome phase. Blue dots indicate responders (n=19) and red
744 dots indicate non-responders (n=7).

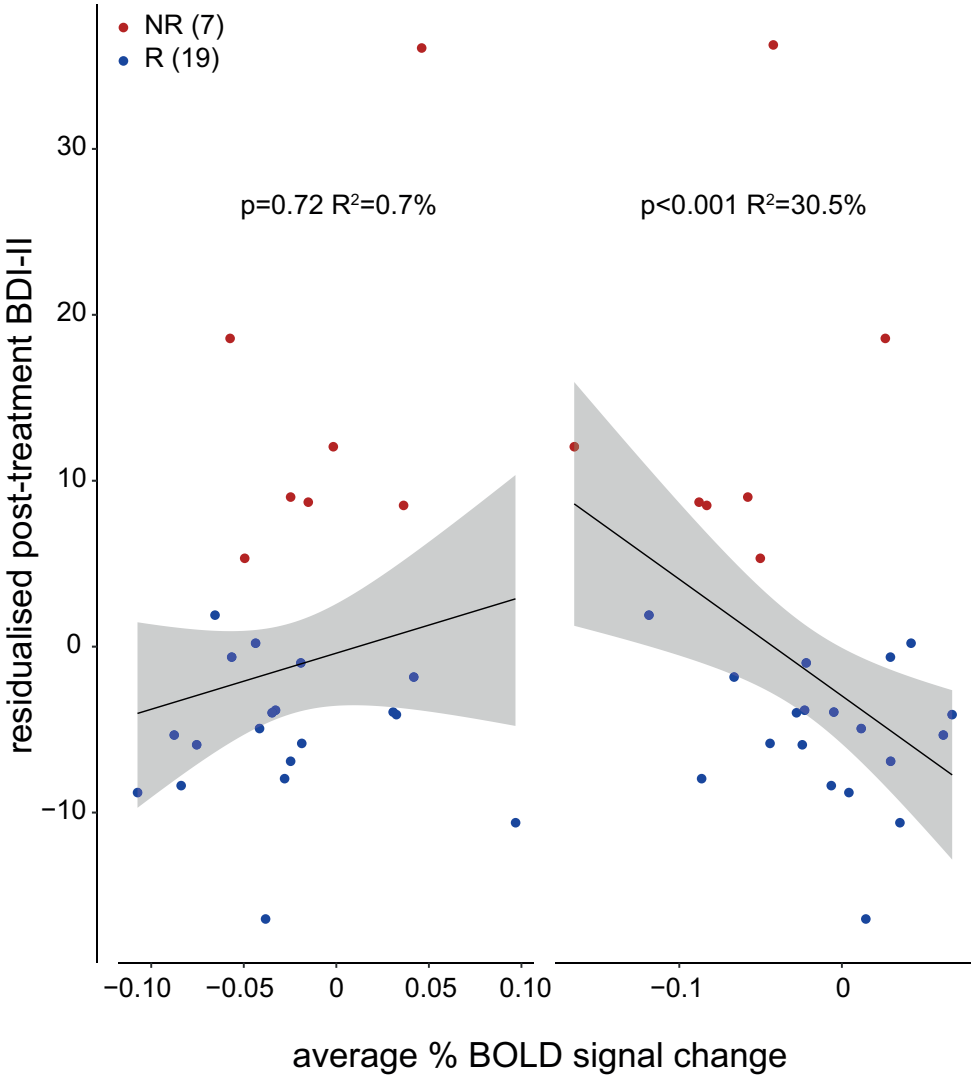

745

746

Supplemental Figure S1. Pre-treatment time course of BOLD percent signal change in the dmPFC without non-completers.

Average feedback-locked BOLD percent signal change ± SEM (blue and red shading) in responders (blue; n=19) and completers non-responders (red; n=7) groups is plotted as a function of feedback valence and congruence. Averages are adjusted for pre-treatment BDI-II score. We performed between-group comparisons over the temporal window shown by the grey shaded box. Between-group differences were robust to response bias during incongruent negative trials (bottom right; $F(1,23.2)=4.99$, $p=0.03$) but not during congruent negative trials (bottom left; $F(1,22.6)=1.23$, $p=0.27$).